

Synthesis, Structural Investigations, and Dielectric Properties of Irradiated Flexible Polymeric Composite Films

To cite this article: M. M. Abdelhamied *et al* 2024 *ECS J. Solid State Sci. Technol.* **13** 063003

View the [article online](#) for updates and enhancements.

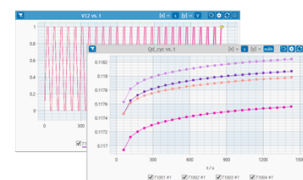
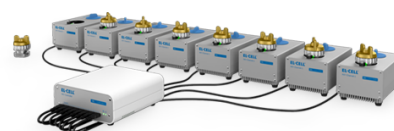
You may also like

- [Green to deep-red emissive carbon dot formation by C⁺ ion implantation on nitrogen beam created self-masked nano-template](#)
Sudip Bhowmick, Joy Mukherjee, Manorama Ghosal et al.
- [Carbon ion beam induced chemical modification and nano-pyramid growth on Si surface](#)
Sudip Bhowmick, Joy Mukherjee, Manorama Ghosal et al.
- [Impacts of Low Energy Oxygen Irradiation on the Dielectric Properties of PVA/TiO₂ Nanocomposite Films](#)
Reem Altujiri, M. M. Abdelhamied, A. Atta et al.

PAT-Tester-x-8 Potentiostat: Modular Solution for Electrochemical Testing!

EL-CELL®
electrochemical test equipment

- ✓ **Flexible Setup with up to 8 Independent Test Channels!**
Each with a fully equipped Potentiostat, Galvanostat and EIS!
- ✓ **Perfect Choice for Small-Scale and Special Purpose Testing!**
Suited for all 3-electrode, optical, dilatometry or force test cells from EL-CELL.
- ✓ **Complete Solution with Extensive Software!**
Plan, conduct and analyze experiments with EL-Software.
- ✓ **Small Footprint, Easy to Setup and Operate!**
Usable inside a glove box. Full multi-user, multi-device control via LAN.



Contact us:

+49 40 79012-734


sales@el-cell.com

www.el-cell.com





Synthesis, Structural Investigations, and Dielectric Properties of Irradiated Flexible Polymeric Composite Films

M. M. Abdelhamied,¹  Reem Altuijri,² A. Atta,^{3,z} and Mohammed Ezzeldien³

¹Radiation Physics Department, National Center for Radiation Research and Technology (NCRRT), Egyptian Atomic Energy Authority (EAEA), Cairo, Egypt

²Department of Physics, College of Science, Princess Nourah bint Abdulrahman University, P.O. Box 84428, Riyadh 11671, Saudi Arabia

³Physics Department, College of Science, Jouf University, Sakaka, Saudi Arabia

In this research, the casting solution manufacturing approach was used to mix polyvinyl alcohol (PVA) and copper oxide (CuO) to create the composite (PVA/CuO). X-ray diffraction analysis and Fourier transform infrared spectroscopy were applied to record the successful fabrications of the composites. Next, argon ion beams at fluencies of 2.5×10^{17} , 5×10^{17} , and 7.5×10^{17} ions.cm⁻² were used to irradiate the composites. In frequencies of 50 Hz to 6 MHz, the dielectric characteristics of PVA/CuO were modified by the ion irradiation. The dielectric constant was enhanced from 39 for unmodified PVA/CuO to 356 for the irradiated composite by 7.5×10^{17} ions.cm⁻², and the conductivity changed from 0.05×10^{-6} S cm⁻¹ to 2.9×10^{-6} S cm⁻¹. However, the potential barrier decreased from 0.24 eV for PVA/CuO to 0.21, 0.16, and 0.15 eV, respectively, for 2.5×10^{17} , 5×10^{17} , and 7.5×10^{17} ions.cm⁻², and the relaxation time decreased from 9.36×10^{-8} sec for PVA/CuO, to 6.58×10^{-8} sec for 7.5×10^{17} ions.cm⁻². The results indicate that the irradiated PVA/CuO nanocomposite can be used in a number of devices such as capacitors and batteries.

© 2024 The Electrochemical Society ("ECS"). Published on behalf of ECS by IOP Publishing Limited. [DOI: [10.1149/2162-8777/ad4f71](https://doi.org/10.1149/2162-8777/ad4f71)]

Manuscript submitted March 22, 2024; revised manuscript received May 10, 2024. Published June 4, 2024.

The last several decades have seen the emergence of polymer nanocomposites as a promising field for study and development because of their special qualities and extensive range of applications.^{1,2} These materials provide a new class of materials with improved physical, thermal, electronic, and optical properties by combining nanoscale fillers, with long chains of repeating subunits, known as polymers.^{3,4} Because of the addition of nanoscale fillers to polymers results in materials with enhanced stiffness, strength, and toughness.^{5,6} This produces materials that are lighter and stronger at the same time, which makes them very desirable for a variety of applications.⁷ Polymer nanocomposites are perfect for usage in the electronics industry since they have improved thermal stabilities in addition to their improved mechanical qualities.⁸

Because of its special qualities and range of uses, PVA is widely utilized, and has become extremely popular across a number of sectors.⁹ PVA is easily manipulated to create films, fibers, and coatings, which makes it a great option for a variety of uses.¹⁰ PVA is a great material for textiles, concrete reinforcement, and packaging because it has good dimensional stability and can be used with other polymers.¹¹ PVA is also ideal for use in agriculture because of its outstanding transparency, strong mechanical strength and gas barrier qualities.¹² CuO nanofiller has been extensively studied for its potential as a catalyst in a variety of chemical processes, including reduction and oxidation.¹³ CuO nanofiller's distinctive structure and large surface area make it useful for uses in chemical synthesis and energy conversion.¹⁴ CuO is a superior option for optical, electrical, and sensing devices due to their low production cost and ideal electrochemical properties.^{15,16}

One of the main advantages of an ion beam irradiation is increase the interfacial contact of nanofillers and the polymer matrix.^{17,18} Additionally, ion irradiation has been shown to be more successful than electrons in the field of particles beam approaches at altering a polymer surface. This is a result of the increased ionization cross-section of the energetic ions as compared to electron. The dispersion and interlocking of the nanofillers inside the polymer matrix can be efficiently promoted by the energetic ions.^{19,20} Ion beams irradiation can affect the nanocomposite's electrical and optical characteristics in addition to its mechanical and thermal properties.²¹ Electrical conductivity qualities can be altered by changing the structure of the

irradiated samples, which opens up new possibilities in industries like electronics, photonics, and sensing. The objective in this study was to present the PVA/CuO composite's synthesis, characterization, and application procedures. The present investigation involved subjecting the composite PVA/CuO films to a range of argon ion beam. The resulting alterations in the composite's structural characteristics were made evident using the XRD and FTIR methods. The dielectric properties of these exposed films were computed. The utilization of these bombarded PVA/CuO films can be applied in dielectric applications as indicated by these outcomes.

Experimental

The used substances; CuO (99.5%) and PVA (MW 79000 g mol⁻¹), were given by Sigma-Aldrich company. The PVA fabricated by dissolving 0.8 gm of PVA for 80 ml in distilled water, with constant stirring to produce a homogenous solution.²² In order to create PVA/CuO films, a solution containing the PVA was mixed with 2.0 weight percent CuO powder utilizing the solution casting process previously discussed.²³ After that, the mixture was constantly swirled for 120 min. To create the films, the PVA/CuO combination was cast into a Petri dish. To facilitate analysis, the films were removed from the Petri plates and cutted into 1.8 cm by 1.8 cm pieces. A thickness gauge (7301 dial thickness gage, Mitutoyo, Japan) was used to measure the produced films average thickness of 50 μ m.

After removal from the Petri dishes, argon beams with fluencies of 2.5×10^{17} , 5.0×10^{17} , and 7.5×10^{17} ions cm⁻² were used to irradiate the produced PVA/CuO films using the ion source, as illustrated in Fig. 1. As we previously described.²⁴ The ionization region, where a plasma is created, and the extraction region, where ions are extracted and accelerated to produce a beam, are the two components of the source. The chamber is surrounded by permanent magnets, and a tiny aperture allows gas to enter. The energy of the extracted ions was 3 keV, the pressure was about 1.3×10^{-4} mbar, and the beam intensity was 145 μ A cm⁻². The XRD (XRD-6000, Shimadzu, Japan) of Cu K α and $\lambda = 1.54056$ Å, was used to examine the structure of the PVA/CuO samples. The produced films' chemical compositions were ascertained by The FTIR (ATI Mattson, England) was used to study the bonding interactions. Using the LCR meter with a frequency in range of 20 Hz to 5.5 MHz, the dielectric characteristics were determined.

^zE-mail: aamahmad@ju.edu.sa

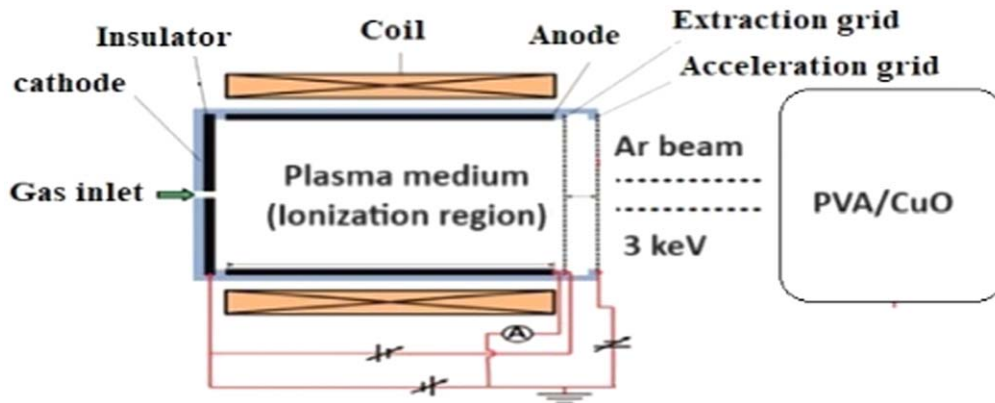


Figure 1. The ion broad ion source with electrical circuit.

Results and Discussion

The SRIM simulating method²⁵ was utilized to record the ion beam interaction with the composite, as shown in Fig. 2. The energy used is of 3 keV argon ions interacted with the PVA/CuO at depths ranging from 0 to 1000 Å. As shown in Fig. 2a, the distribution of the argon ion beam forms a path for the bombarded ions in the composite PVA/CuO. Following the irradiation of the ion beam with

the target, the penetrating argon ions distributed within a mean range of 5.6 nm. The atoms of carbon and hydrogen recoil when they come into contact with argon ions. Figure 2b illustrates the energy absorbed by the target atoms; this energy allowed the recoiled atoms to escape their locations within the structure and interact with other atoms. Figure 2c depicts the target damage caused by the collisions events of the argon ions colliding with the target

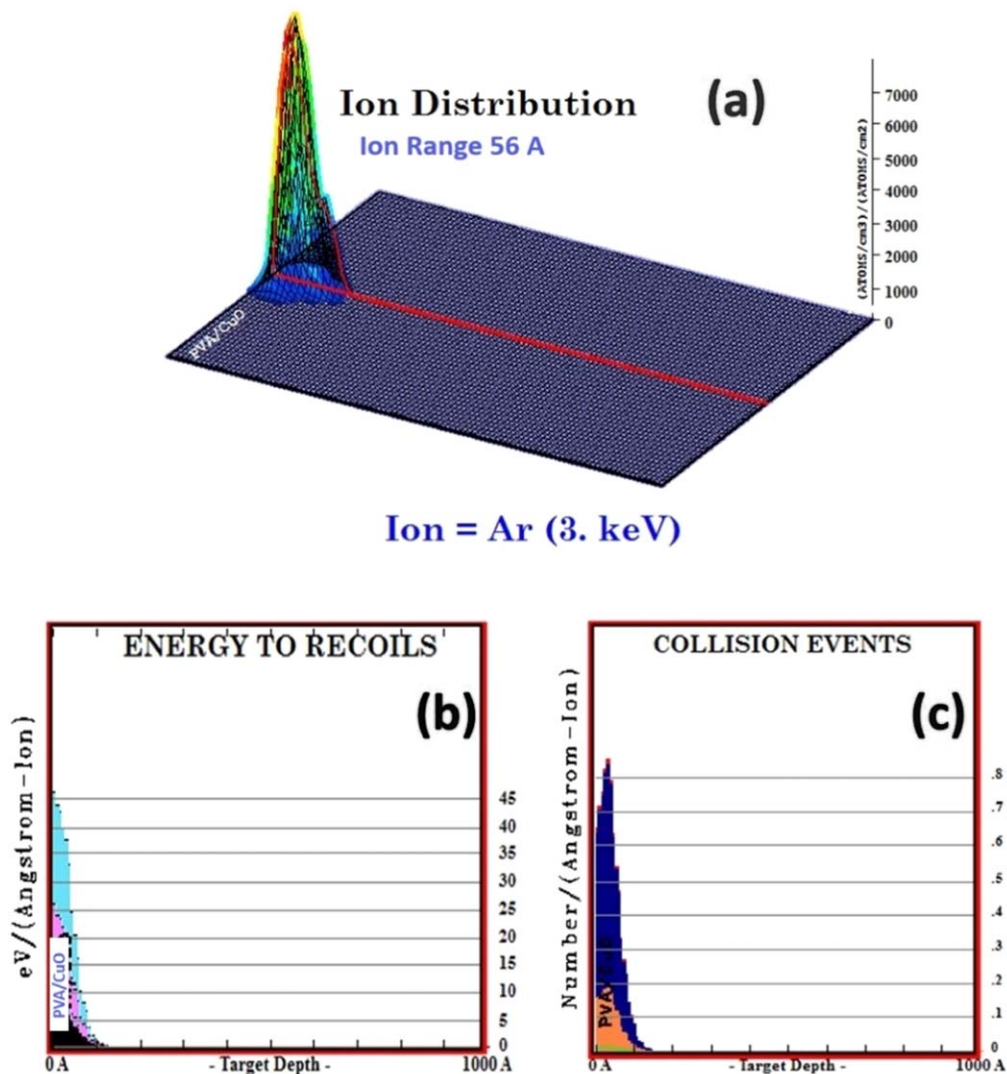


Figure 2. (a) Ion distributions of ion beam with PVA/CuO, (b) Recoiled atoms distribution of ions by PVA/CuO, and (c) Collision of argon ions by PVA/CuO.

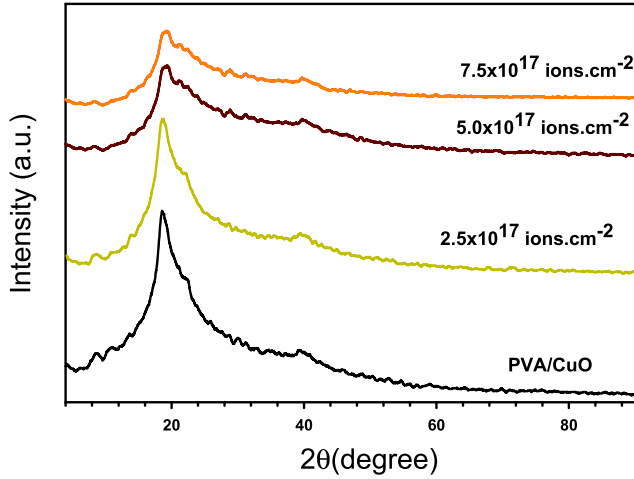


Figure 3. XRD of pure and treated PVA/CuO films.

vacancies. The target material was expected to develop interface or near-surface defects when exposed to ion beams. Ion bombardment can alter targets due to certain defects, such as vacancies and interstitial atoms.

The XRD of the pristine and bombarded PVA/CuO is displayed in Fig. 3 in the 2θ range of 4° – 88° . The PVA/CuO formation is shown by peak of 2θ at 19.6° for PVA (001) diffraction and an additional peak at 39° for CuO. Moreover, it is noted that scission and radical production resulted in a drop in the intensity of the PVA with irradiation. Additionally, after exposed to the ion beam, a slight shifting of the principal peaks occurred, which, was brought by the formation of crystal structure defects. According to,²⁶ the crystallite size (D) is given by.

$$D = \frac{0.94\lambda}{\beta \cos \theta} \quad [1]$$

Further, the diameter (R) was computed by Eq. 2.²⁷

$$R = \frac{\lambda}{\sin \beta \cos 2\theta} \quad [2]$$

After irradiating PVA/CuO by 7.5×10^{17} ions cm^{-2} , the D and R dropped from 17.4 nm and 230 μm for the PVA/CuO film to 13.1 nm and 174 μm , correspondingly. The dislocation density (δ) is calculated by.²⁷

$$\delta = \frac{1}{D^2} \quad [3]$$

The dislocation density improved from $3.11 \times 10^{-3} \text{ nm}^{-2}$ for PVA/CuO to $5.82 \times 10^{-3} \text{ nm}^{-2}$ for 7.5×10^{17} ions cm^{-2} , as listed in Table I. By using the Stokes-Wilson equalization, the lattice strain (ϵ) was calculated by Eq. 4.²⁸

$$\epsilon = \frac{\beta}{4 \tan \theta} \quad [4]$$

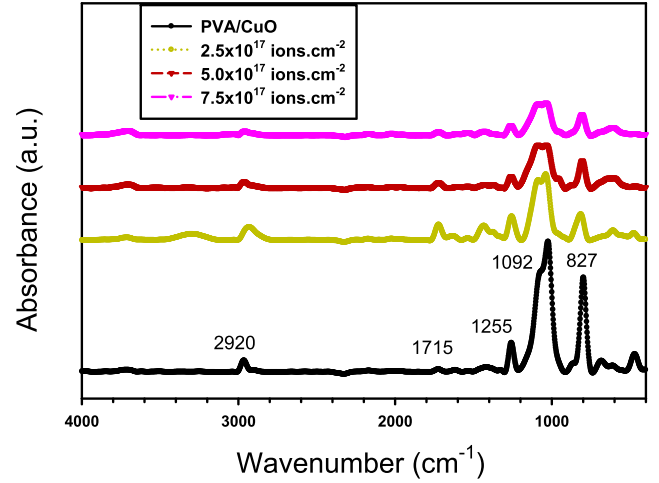


Figure 4. FTIR of pristine and bombarded PVA/CuO films.

The strain ϵ grew from 0.075×10^{-3} for the PVA/CuO film to 0.10×10^{-3} for the 7.5×10^{17} ions cm^{-2} bombarded composites. Lastly, the distortion coefficients (g) of the pristine and bombarded sheets were calculated by Eq. 5.²⁸

$$g = \frac{\beta}{\tan(\theta)} \quad [5]$$

Following radiation exposure by 7.5×10^{17} ions cm^{-2} , the g of the PVA/CuO film rose from 11.1% to 16.3%, confirming the disordered network in the irradiated composites.

The FT-IR spectrum of PVA/CuO is shown in Fig. 4. The stretching band of CH_2 is for the peaks at 2920 cm^{-1} . The peaks for $\text{C}=\text{O}$ is appear at 1715 cm^{-1} , and the peak at 1255 cm^{-1} is for $\text{C}-\text{H}$ vibration. The asymmetric vibrations of $\text{C}-\text{O}$ and $\text{C}-\text{C}$ are associated with the peaks at 1092 and 827 cm^{-1} , correspondingly. The peak at nearly 3200 cm^{-1} is for hydrogen bonds of the OH groups for the composite PVA/CuO. Due to the chemical linkages in the polymer nanocomposite, the intensity of this spectrum was reduced for the bombarded samples relative to that of the PVA/CuO. Another probable reason for the drop in peak intensity could be the production of free radicals, which induce electrons to hopping of valence to conduction states.²⁹

The irradiated composite showed changes in peak intensity, showing that ion irradiation affected the composite PVA/CuO bonding interaction. The figure shows that the broad peak (3100 – 3400 cm^{-1}) was moved by irradiation, indicating the bonding of the oxygen CuO and the OH group of PVA. The PVA/CuO sample showed just a minor shift in peak intensity and location when subjected to ion radiation. In addition, there was no noticeable change in the carbonyl group ($\text{C}=\text{O}$) at 1715 cm^{-1} , suggesting that the composite PVA/CuO films is stable under irradiation.

Figure 5a investigate the SEM images of the untreated composite PVA/CuO, and Figs. 5b–5d displays the images of the irradiated samples. Figure 5a shows the microstructures of the PVA/CuO film as a smooth and regular surface. As shown in Figs. 5b–5d for irradiated composites with fluencies of 2.5×10^{17} , 5×10^{17} , and

Table I. The structural parameters of the pristine and treated PVA/CuO films.

The samples	D [nm]	R [μm]	$\delta [10^{-3}] (\text{nm}^{-2})$	$\epsilon [10^{-3}]$	g (%)
PVA/CuO	17.1	226	3.41	0.075	11.1
2.5×10^{17} ions cm^{-2}	15.6	208	4.11	0.082	11.4
5.0×10^{17} ions cm^{-2}	14.2	190	4.95	0.094	14.5
7.5×10^{17} ions cm^{-2}	13.1	174	5.82	0.101	16.3

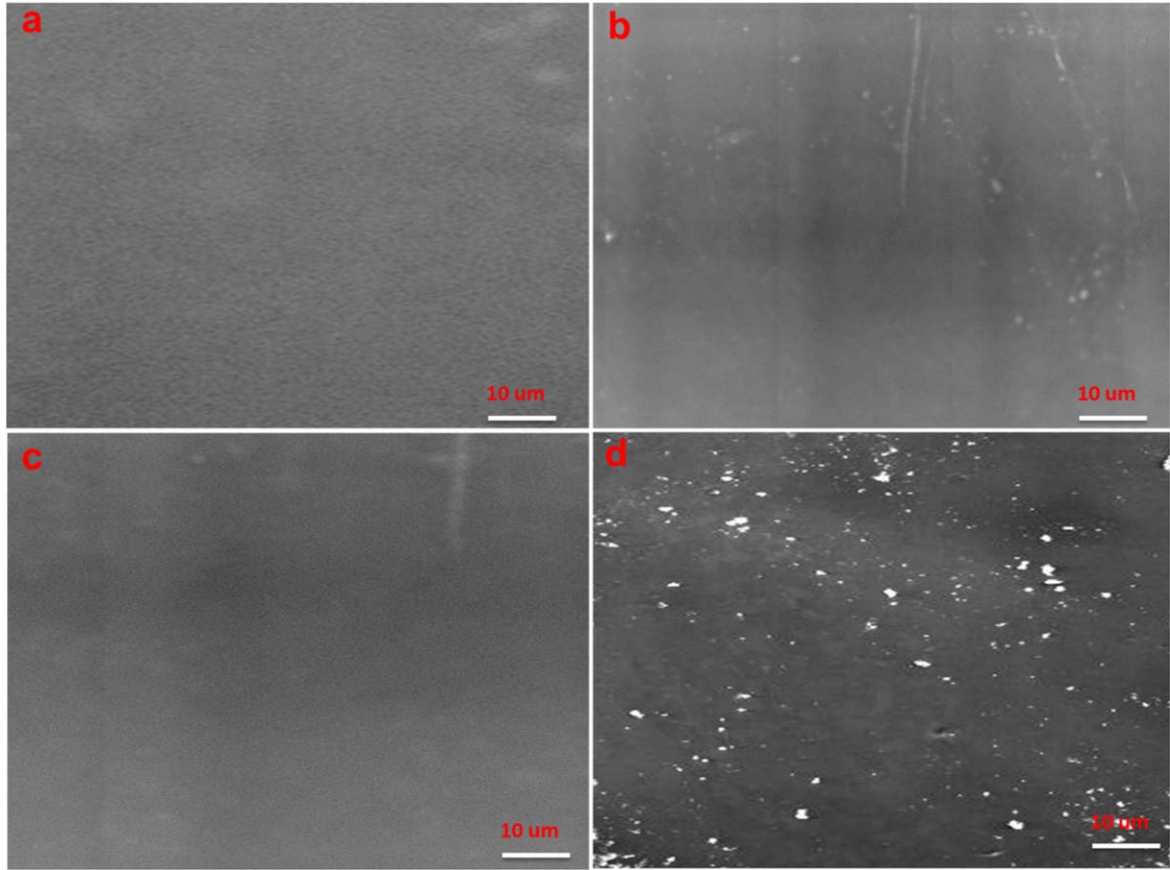


Figure 5. SEM of (a) PVA/CuO, (b) 2.5×10^{17} ions.cm⁻², (c) 5×10^{17} ions.cm⁻² and (d) 7.5×10^{17} ions.cm⁻².

7.5×10^{17} ions.cm⁻², correspondingly, were found in close contact to each other. This is because shorter inter-particles distances were induced by irradiation, with more rough fracture surfaces. The irradiated films also showed no signs of surface cracking in the images, which is consistent with the results of the FTIR analyses, suggesting that the films were more stable after ion irradiation.

Analyzing the dielectric is a very sensitive way of finding relevant details concerning a composites structure. The dielectric permittivity (ϵ^*) is given by Eq. 6.³⁰

$$\epsilon^* = \epsilon' - i\epsilon'' \quad [6]$$

The real constant ϵ' can be estimated by Eq. 7.³⁰

$$\epsilon' = \frac{c \cdot t}{\epsilon_0 \cdot A} \quad [7]$$

where A is the surface area, t is the thickness and c is the capacitance of the film. Figure 6 shows the ϵ' for both bombarded and virgin PVA/CuO, with respect to the frequency. At low frequencies, the ϵ' for all samples were decreasing rapidly with increasing frequency, and at high frequency (above 3 MHz), it approached to a constant. This could be due to the fact that the dipoles were not given a enough amount of time to orient themselves.^{31,32} According to Table II the ϵ' at frequency 50 Hz rose from 39 for pure PVA/CuO to 71 after a exposed to 2.5×10^{17} ions.cm⁻² to 356 for 7.5×10^{17} ions.cm⁻². Due to the polarization and imperfections, the irradiated films' dielectric constant were improved.³³

The dielectric loss, ϵ'' , is given by Eq. 8.³⁴

$$\epsilon'' = \epsilon' \tan\delta \quad [8]$$

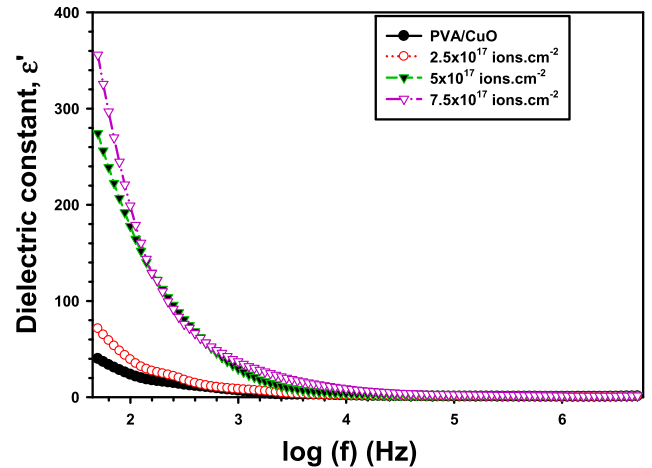


Figure 6. The ϵ' with frequency of pristine and bombarded PVA/CuO.

Figure 7 shows the plots of ϵ'' against frequency of the pure and treated PVA/CuO composites. In particular, as the frequency rose, the ϵ'' declined, which is due to a decrease in the space charge polarization contributions.³⁵ In addition, faults resulting from chain scissioning caused a very substantial increase in ϵ'' by ion beam at various dosages of irradiation. As indicated in Table II, the ϵ'' rose from 19 for unirradiated PVA/CuO to 72 for 2.5×10^{17} ions.cm⁻² and 1042 for 7.5×10^{17} ions.cm⁻². The cause of this rise was due to the interfacial polarization with the ion irradiation at the nonconductor/conductor contacts.³⁶

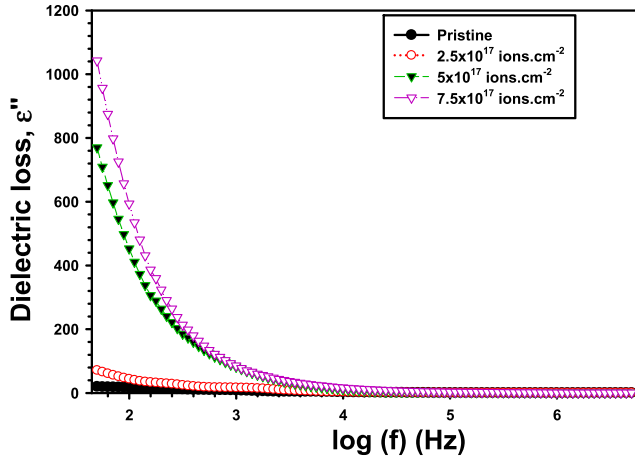


Figure 7. The ϵ'' changes with frequency of the electric field of pure and treated PVA/CuO.

The modulus (M^*) is determine by.³⁷

$$M^* = \frac{1}{\epsilon^*} = M' + iM'' \quad [9]$$

where M' and M'' are the real and imaginary complex moduli, respectively, and ϵ^* is the complex permittivity. The M' and M'' were given by Eqs. 10 and 11.³⁸

$$M' = \frac{\epsilon'}{\epsilon'^2 + \epsilon''^2} \quad [10]$$

$$M'' = \epsilon''/(\epsilon'^2 + \epsilon''^2) \quad [11]$$

Figure 8 displays M' with the frequency of the pristine and the bombarded PVA/CuO sheets by 2.5×10^{17} , 5×10^{17} , and 7.5×10^{17} ions.cm⁻² of argon beam. The M' was very small in the low frequency zone, as shown in Fig. 8. The M' rose with the frequency, reaching a maximum value and then decreased at greater frequencies.³⁹ This phenomenon occurs because electrical dipoles in polymers are more likely to align at low frequencies than at high-frequencies.⁴⁰ According to Table II, for un-irradiated PVA/CuO, the M' value at 50 Hz decreased from 20.1×10^{-3} to 7.2×10^{-3} for 2.5×10^{17} ions.cm⁻² and to 0.32×10^{-3} for 7.5×10^{17} ions.cm⁻². The modulus drops after treatment because the charge localization efficiency was enhanced by the dipolar contribution of charge carriers. Furthermore, this is because ion irradiation changes the composite structure and increases the defect density in the films that are exposed to irradiation.

Figure 9 illustrates how the M'' with frequency in both the irradiated and pure PVA/CuO films. The figure displays a 2 peaks of M'' that indicates the occurrence of a relaxation behavior. The M'' is near to zero value at the lower frequencies and by increasing the frequency, it enhanced to reach a maximum value. The M'' decreased from 10.4×10^{-3} for un-irradiated PVA/CuO to 7.5×10^{-3} for 2.5×10^{17} ions.cm⁻² and to 0.88×10^{-3} for 7.5×10^{17} ions.cm⁻² at 50 Hz. The relaxation time (τ_r) is given by Eq. 12.⁴⁰

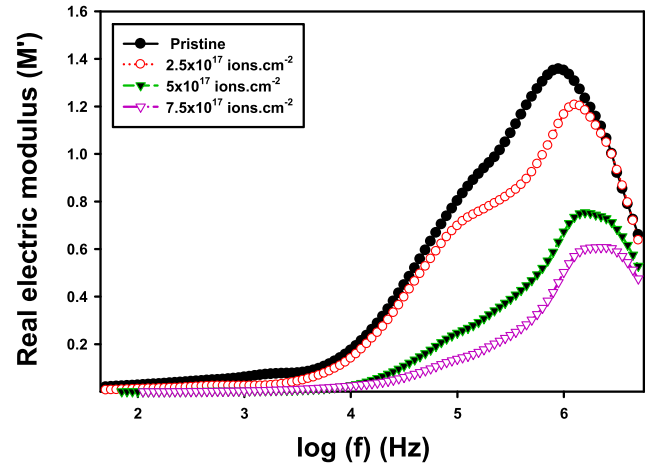


Figure 8. The M' vs frequency of pristine and bombarded PVA/CuO.

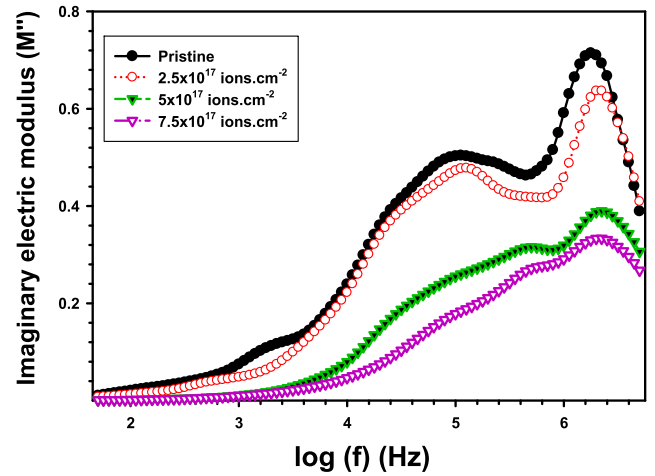


Figure 9. The M'' with frequency of pure and treated PVA/CuO films.

$$\tau_s = \frac{1}{2\pi f_p} \quad [12]$$

The chain relaxation period corresponding to the peak of frequency f_p is denoted by τ_s . When PVA/CuO is exposed to radiation, its intensity peak shifts to a greater frequency, indicating a reduction in the relaxation time (τ_r). The relaxation time was 9.36×10^{-8} sec for PVA/CuO, decreased to 7.96×10^{-8} sec, 7.23×10^{-8} sec, and to 6.58×10^{-8} sec for 2.5×10^{17} , 5×10^{17} , and 7.5×10^{17} ions.cm⁻². The exposure to radiation reduced the relaxation time, which accounts for the drop in τ_s of modified PVA/CuO. Additionally, exposure lowers τ_s , due to the conductivity rising with greater mobility.⁴¹

Table II. ϵ' , ϵ'' , M' , M'' , σ_{ac} and U of pristine and bombarded PVA/CuO. at 50 Hz.

	ϵ'	ϵ''	M'	M''	σ_{ac} (S/cm)	U (J/m ³)
PVA/CuO	39	19	20.1×10^{-3}	10.4×10^{-3}	0.05×10^{-6}	1.77×10^{-4}
2.5×10^{17} ions cm ⁻²	71	72	7.2×10^{-3}	7.5×10^{-3}	0.19×10^{-6}	3.16×10^{-6}
5.0×10^{17} ions cm ⁻²	274	769	0.4×10^{-3}	1.19×10^{-3}	2.16×10^{-6}	12.1×10^{-4}
7.5×10^{17} ions cm ⁻²	356	1042	0.32×10^{-3}	0.88×10^{-3}	2.94×10^{-6}	15.7×10^{-4}

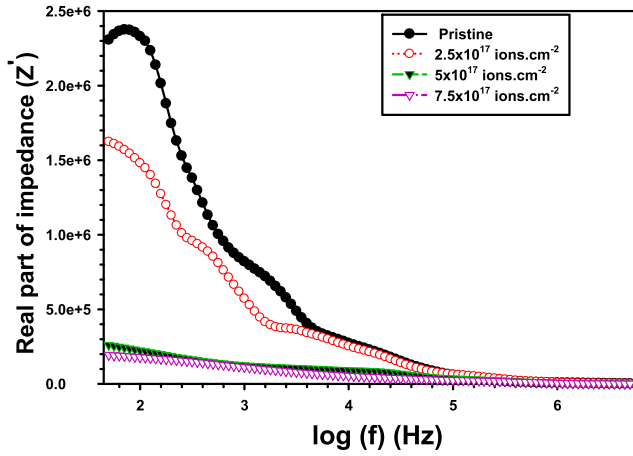


Figure 10. The Z' vs frequency of pristine and bombarded PVA/CuO at different fluencies.

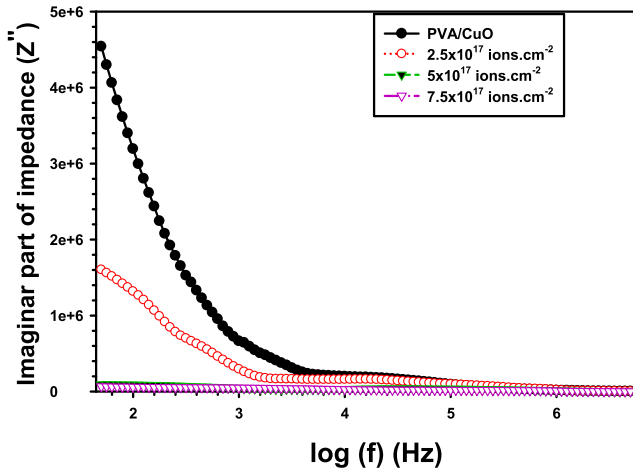


Figure 11. The Z'' vs frequency of pristine and bombarded PVA/CuO at different fluencies.

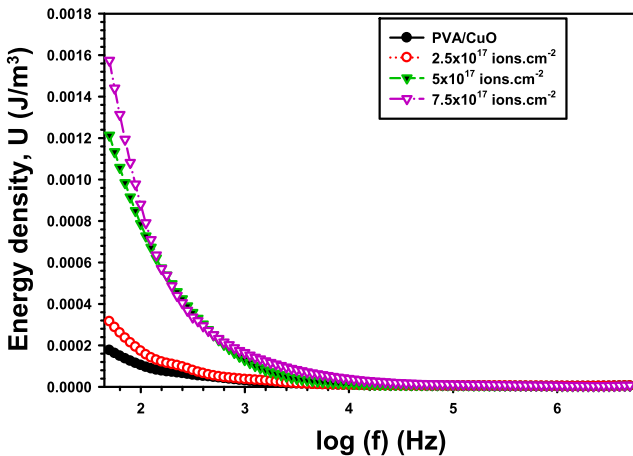


Figure 12. The U with frequency of pristine and bombarded PVA/CuO.

Furthermore, the complex impedance, Z^* , is given by.⁴²

$$Z^* = Z' + iZ'' \quad [13]$$

The real impedance is represented by Z' , which provides information on the resistive fraction, and the reactance portion is

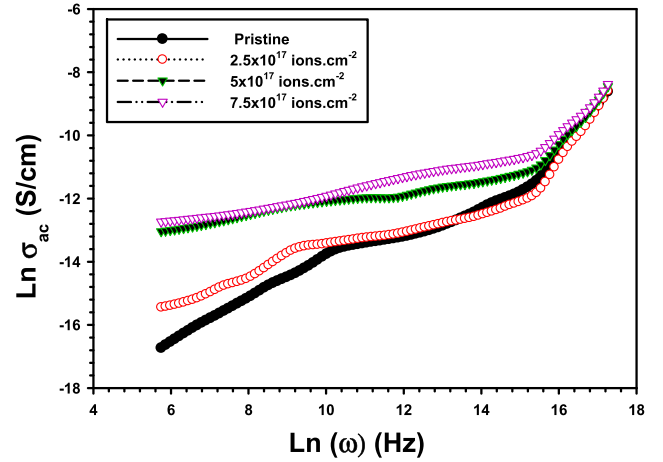


Figure 13. The σ_{ac} vs frequency of pristine and bombarded PVA/CuO.

given by Z'' . As shown in Fig. 10, the magnitudes of Z' for the films fell as the frequency increased and became nearly zero value at higher frequencies. As previously mentioned, as ion beam irradiation rises, the Z' continuously drop.

Figure 11 displays the variation in Z'' of both the bombarded and unirradiated PVA/CuO nanocomposite sheets with respect to frequency. It is evident that the Z'' exhibit the same decreasing tendency with frequency. Moreover, because the free carriers were increased, the Z' decrease by irradiation.⁴³ The CuO is responsible for the occurrence of dielectric relaxation peaks in the Z' and Z'' , of the pristine PVA/CuO and the irradiated $2.5 \times 10^{17} \text{ ions.cm}^{-2}$, confirming that the composites were suitable for energy storage devices.⁴⁴ As previously mentioned, with increasing irradiation magnitude, the values of Z' and Z'' fall because there are more free charge carriers. This is due to increased free charge availability, which improves conduction and maintains impedance.

The energy density (U) was estimated for practical applications by Eq. 14.⁴⁵

$$U = \frac{1}{2} \epsilon' \epsilon_0 E^2 \quad [14]$$

The U is changes with frequency, as given in Fig. 12. PVA/CuO exhibited an energy density of $1.77 \times 10^{-4} \text{ J/m}^3$ for the untreated sample as shown in Table II, which was modified to $3.16 \times 10^{-4} \text{ J m}^{-3}$ at $2.5 \times 10^{17} \text{ ions.cm}^{-2}$ and to $15.7 \times 10^{-4} \text{ J m}^{-3}$ at $7.5 \times 10^{17} \text{ ions.cm}^{-2}$. This is due to, when the composites were exposed to ion beam irradiation, the charges were transferred more quickly. The findings validate that ion treatment of PVA/CuO enhanced the dielectric characteristics of the energy storage.

The conductivity, σ_{ac} , is given by Eq. 15.⁴⁶

$$\sigma_{ac} = 2\pi f \epsilon_0 \epsilon'' \quad [15]$$

Figure 13 illustrates the change in σ_{ac} of both bombarded and pure PVA/CuO composite films with frequency. Interestingly, for every sample, the σ_{ac} rises with frequency; this is because the variations of the applied electric fields changes the charge carriers.^{47,48} To be more specific, the σ_{ac} at frequency 50 Hz increased from $0.05 \times 10^{-6} \text{ S/cm}$ for the PVA/CuO to $2.94 \times 10^{-6} \text{ S cm}^{-1}$ at $7.5 \times 10^{17} \text{ ions cm}^{-2}$. The chain scissoring, which increases the speed of ionic movement, was the reason for this rise in σ_{ac} due to rising ion beam impacts. Additionally, as the ion beam effects increase, the values of σ_{ac} conductivity is increased due to the induced free carriers by ion irradiation.

The highest achievable potential barrier, W_M , was estimated by utilizing the subsequent Eq. 16.⁴⁹

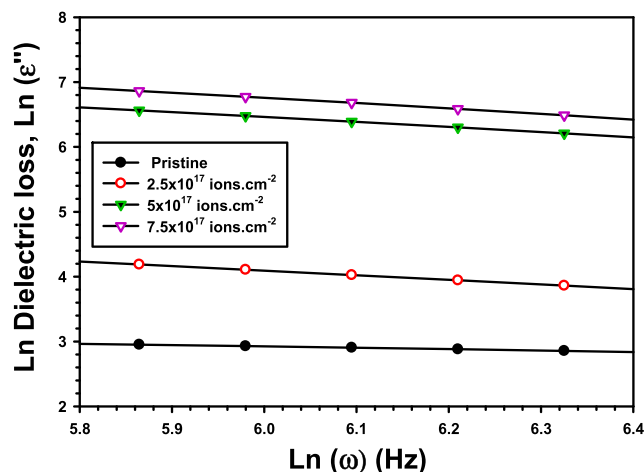


Figure 14. Ln (ϵ'') vs Ln (ω) of pure and treated PVA/CuO films.

$$W_m = \frac{-4k_B T}{m} \quad [16]$$

The temperature is T and m is estimated by the sloping curves of Ln (ϵ'') against Ln (ω), which is illustrated in Fig. 14, according to the Eq. 17.⁵⁰

$$\epsilon'' = A\omega^m \quad [17]$$

The derived W_m decreased from 0.24 eV for PVA/CuO, to 0.21 eV, 0.16 eV, and 0.15 eV, correspondingly for the 2.5×10^{17} ions.cm⁻², 5×10^{17} ions.cm⁻² and 7.5×10^{17} ions.cm⁻² samples. Therefore, the treatment of the films improved their electrical conductivity, as seen by the reduction in the W_m value.

Conclusions

The handmade ion beam source was applied to effectively irradiate the films. PVA/CuO composite sheet manufacturing was confirmed by XRD and FTIR. The XRD examined the amorphicity of the bombarded PVA/CuO, which rose with ion exposure as a result of variations in dislocation density and crystallite size. Exposure to various ion beam fluencies increased the conductivity. The impedance characteristics of the bombarded PVA/CuO film were revealed by the energy density, which increased from 1.77×10^{-4} J/m³ for the pure composite to 15.7×10^{-4} J/m³ for the irradiated samples. The relaxation time reduced from 9.36×10^{-8} sec for PVA/CuO to 7.96×10^{-8} sec, 7.23×10^{-8} sec, and to 6.58×10^{-8} sec for 2.5×10^{17} ions.cm⁻², 5×10^{17} ions.cm⁻² and 7.5×10^{17} ions.cm⁻². In contrast, the dielectric loss rose with increasing irradiation from 19 for PVA/CuO to 1042 for the irradiated film. The findings of this work open up new possibilities for diverse dielectric devices, such as microelectronic devices, batteries, and supercapacitors.

Acknowledgments

Princess Nourah bint Abdulrahman University Researchers Supporting Project number (PNURSP2024R399), Princess Nourah bint Abdulrahman University, Riyadh, Saudi Arabia.

ORCID

M. M. Abdelhamied  <https://orcid.org/0009-0003-3439-1791>

References

1. A. Alshahrie, S. Saini, P. M.-Z. Hasan, A. A. Al-Ghamdi, A. M. Quraishi, A. Alsulami, and P. A. Alvi, "Biocompatible Poly (Vinyl Alcohol)-copper oxide-

graphene oxide (PVA-CuO-GO) nanocomposites: synthesis, structural and optical properties." *Sci. of Advan. Mat.*, **15**, 412 (2023).

2. A. M. Abd-Elnaem, M. Rashad, T. A. Hanafy, and N. M. Shaalan, "Improvement of optical properties of functionalized polyvinyl alcohol-zinc oxide hybrid nanocomposites for wide UV optoelectronic applications." *J. Inorg. Organomet. Polym. Mater.*, **33**, 1 (2023).
3. A. Atta, S. Lotfy, and E. Abdeltwab, "Dielectric properties of irradiated polymer/multiwalled carbon nanotube and its amino functionalized form." *J. of Appl. Polym. Sci.*, **135**, 46647 (2018).
4. A. Abdel-Galil, A. Atta, and M. R. Balboul, "Effect of low-energy oxygen ion beam treatment on the structural and physical properties of ZnO thin films." *Surf. Rev. Lett.*, **27**, 2050019 (2020).
5. M. M. Abdelhamied, A. Atta, A. M. Abdelreheem, A. T. M. Farag, and M. M. El Okr, "Synthesis and optical properties of PVA/PANI/Ag nanocomposite films." *J. Mater Sci-Mater El.*, **31**, 22629 (2020).
6. A. Atta and E. Abdeltwab, "Influence of ion irradiation on the surface properties of silver-coated flexible PDMS polymeric films." *Braz. J. Phys.*, **52**, 1 (2020).
7. M. M. Abdelhamied, A. Atta, A. M. Abdelreheem, A. T. M. Farag, and M. A. El Sherbiny, "Oxygen ion induced variations in the structural and Linear/Nonlinear optical properties of the PVA/PANI/Ag nanocomposite film." *Inorg. Chem. Commun.*, **133**, 108926 (2021).
8. A. Atta, M. M. Abdelhamied, A. M. Abdelreheem, and N. A. Althubiti, "Effects of polyaniline and silver nanoparticles on the structural characteristics and electrical properties of methylcellulose polymeric films." *Inorg. Chem. Commun.*, **135**, 109085 (2022).
9. E. Abdeltwab and A. Atta, "Structural and electrical properties of irradiated flexible ZnO/PVA nanocomposite films." *Surf Innovations*, **40**, 1 (2021).
10. A. Atta, A. M. Abdel Reheem, and E. Abdeltwab, "Ion beam irradiation effects on surface morphology and optical properties of ZnO/PVA composites." *Surf. Rev. Lett.*, **27**, 1950214 (2020).
11. S. Lotfy, A. Atta, and E. Abdeltwab, "Comparative study of gamma and ion beam irradiation of polymeric nanocomposite on electrical conductivity." *J. Appl. Polym. Sci.*, **135**, 46146 (2018).
12. M. M. Abdelhamied, A. M. Abdelreheem, and A. Atta, "Influence of ion beam and silver nanoparticles on dielectric properties of flexible PVA/PANI polymer composite films." *Plast. Rubber Compos.*, **51**, 1 (2021).
13. R. K. Sendi, N. Al-Harbi, A. Atta, M. Rabia, and M. M. Abdelhamied, "Copper oxide and copper nanoparticles insertion within a PPY matrix for photodetector applications." *Opt. Quantum Electron.*, **55**, 956 (2023).
14. M. M. Abdelhamied, A. Atta, B. M. Alotaibi, N. Al-Harbi, A. M.-A. Henaish, and M. Rabia, "Synthesis of flexible polymer nanocomposites based on methyl cellulose/copper oxide with desired dielectric properties for electrical applications." *Inorg. Chem. Commun.*, **157**, 111245 (2023).
15. A. Atta, E. Abdeltwab, H. Negm, A. H. Alshammari, M. M. Abdelhamied, A. M. Ahmed, and M. Rabia, "Boost the photocatalytic hydrogen production of the nanocomposites conducting polypyrrole modified with metal oxide (CuO)." *Phys. Scr.*, **98**, 095916 (2023).
16. P. M.-Z. Hasan, S. Saini, A. A. Melaibari, N. S. Leel, R. Darwesh, A. M. Quraishi, and P. A. Alvi, "Tunable optical and structural characteristics with improved electrical properties of (PVA-GO-CuO) eco-friendly-polymer nanocomposites and their DFT study." *Diamond Relat Mater.*, **140**, 110425 (2023).
17. N. A. Althubiti, A. Atta, N. Al-Harbi, R. K. Sendi, and M. M. Abdelhamied, "Structural, characterization and linear/nonlinear optical properties of oxygen beam irradiated PEO/NiO composite films." *Opt. Quantum Electron.*, **55**, 348 (2023).
18. N. A. Althubiti, N. Al-Harbi, R. K. Sendi, A. Atta, and A. M. Henaish, "Surface characterization and electrical properties of low energy irradiated PANI/PbS polymeric nanocomposite materials." *Inorg.*, **11**, 74 (2023).
19. N. A. Althubiti, M. M. Abdelhamied, A. M. Abdelreheem, and A. Atta, "Oxygen irradiation induced modification on the linear and nonlinear optical behavior of flexible MC/PANI/Ag polymeric nanocomposite films." *Inorg. Chem. Commun.*, **137**, 109229 (2022).
20. A. Atta, N. Al-Harbi, M. A.-M. Uosif, and E. Abdeltwab, "Structural characteristics and dielectric properties of irradiated polyvinyl alcohol/sodium iodide composite films." *Inorg. Chem. Commun.*, **159**, 111651 (2024).
21. A. Atta, B. M. Alotaibi, and M. M. Abdelhamied, "Structural characteristics and optical properties of methylcellulose/polyaniline films modified by low energy oxygen irradiation." *Inorg. Chem. Commun.*, **141**, 109502 (2022).
22. N. A. Althubiti, A. Atta, B. M. Alotaibi, and M. M. Abdelhamied, "Structural and dielectric properties of ion beam irradiated polymer/silver composite films." *Surf Innovations*, **11**, 90 (2022).
23. Y. Ahmadian, A. Bakravi, H. Hashemi, and H. Namazi, "Synthesis of polyvinyl alcohol/CuO nanocomposite hydrogel and its application as drug delivery agent." *Polym. Bull.*, **76**, 1967 (2019).
24. A. Atta, H. M. Abdel-Hamid, Y. H. A. Fawzy, and M. M. El-Okr, "Characterization and optimization of low-energy broad-beam ion source." *Emerging Mater Res.*, **8**, 354 (2019).
25. J. F. Ziegler, M. D. Ziegler, and J. P. Biersack, "SRIM-The stopping and range of ions in matter." *Nucl. Instrum. Methods Phys. Res., Sect. B*, **268**, 1818 (2010).
26. M. A. El-Kader, M. T. Elabbasy, A. A. Adeboye, and A. A. Menazea, "Nanocomposite of PVA/PVP blend incorporated by copper oxide nanoparticles via nanosecond laser ablation for antibacterial activity enhancement." *Polym. Bull.*, **79**, 1 (2021).
27. R. G. Solanki, P. Rajaram, and P. K. Bajpai, "Growth, characterization and estimation of lattice strain and size in CdS nanoparticles: X-ray peak profile analysis." *Indian J. Phys.*, **92**, 595 (2018).

28. Z. Zare-Akbari, H. Farhadnejad, B. Furughi-Nia, S. Abedin, M. Yadollahi, and M. Khorsand-Ghayeni, "PH-sensitive bionanocomposite hydrogel beads based on carboxymethyl cellulose/ZnO nanoparticle as drug carrier." *Int. J. Biol. Macromol.*, **93**, 1317 (2016).
29. M. T. Khorasani, A. Joorabloo, A. Moghaddam, H. Shamsi, and Z. MansooriMoghadam, "Incorporation of ZnO nanoparticles into heparinised polyvinyl alcohol/chitosan hydrogels for wound dressing application." *Int. J. Biol. Macromol.*, **114**, 1203 (2018).
30. A. Atta, "Enhanced dielectric properties of flexible Cu/polymer nanocomposite films." *Surf Innovations*, **9**, 17 (2020).
31. A. Agrawal and A. Satapathy, "Thermal and dielectric behaviour of polypropylene composites reinforced with ceramic fillers." *J Mater Sci-Mater El*, **26**, 103 (2015).
32. M. Sharma, A. Gaur, and J. K. Quamara, "Effect of 80 MeV O⁶⁺ ion irradiation on structural, morphological, dielectric, and ferroelectric properties of (1-x) PVDF/(x) BaTiO₃ nanocomposites." *Ionics*, **26**, 471 (2020).
33. C. Gavade, N. L. Singh, and P. K. Khanna, "Optical and dielectric properties of ion beam irradiated Ag/polymethyl methacrylate nanocomposites." *J. Nanosci. Nanotechnol.*, **14**, 5911 (2014).
34. S. B. Aziz, M. A. Brza, and P. A. Mohamed, "Increase of metallic silver nanoparticles in Chitosan: AgNt based polymer electrolytes incorporated with alumina filler." *Results Phys*, **13**, 102326 (2019).
35. Y. H. A. Fawzy, H. M. Abdel-Hamid, M. M. El-Okri, and A. Atta, "Structural, optical and electrical properties of PET polymer films modified by low energy Ar⁺ ion beams." *Surf. Rev. Lett.*, **25**, 1850066 (2018).
36. A. Abdel-Galil, H. E. Ali, A. Atta, and M. R. Balboul, "Influence of nanostructured TiO₂ additives on some physical characteristics of carboxymethyl cellulose (CMC)." *J Radiat Res Appl Sci*, **7**, 36 (2014).
37. I. Latif, E. E. AL-Abodi, D. H. Badri, and J. Al Khafagi, "Preparation, characterization and electrical study of (carboxymethylated polyvinyl alcohol/ ZnO) nanocomposites." *Science Am J Potato Polym Sci*, **2**, 135 (2012).
38. G. A. M. Amin and M. H. Abd-El Salam, "Optical, dielectric and electrical properties of PVA doped with Sn nanoparticles." *Mater. Res. Express*, **1**, 025024 (2014).
39. P. Dhatarwal, S. Choudhary, and R. J. Sengwa, "Dielectric and optical properties of alumina and silica nanoparticles dispersed poly (methyl methacrylate) matrix-based nanocomposites for advanced polymer technologies." *J. Polym. Res.*, **28**, 1 (2021).
40. R. Thangarasu, N. Senthilkumar, and B. Babu, "Structural, optical, morphological and electrical properties of V2O5 nanorods and Its Ag/n-V2O5/p-Si/Ag diode application." *J Adv Phys*, **7**, 312 (2018).
41. R. Gupta and R. Kumar, "Influence of low energy ion beam implantation on Cu nanowires synthesized using scaffold-based electrodeposition." *Nano-Structures & Nano-Objects*, **18**, 100318 (2019).
42. G. Sahu, M. Das, M. Yadav, B. P. Sahoo, and J. Tripathy, "Dielectric relaxation behavior of silver nanoparticles and graphene oxide embedded poly (vinyl alcohol) nanocomposite film: an effect of ionic liquid and temperature." *Polym.*, **12**, 374 (2020).
43. S. Atiq, M. Majeed, and A. Ahmad, "Synthesis and investigation of structural, morphological, magnetic, dielectric and impedance spectroscopic characteristics of Ni-Zn ferrite nanoparticles." *Ceram. Int.*, **43**, 2486 (2017).
44. A. M. Abdel Reheem, A. Atta, and T. A. Afify, "Optical and electrical properties of argon ion beam irradiated PVA/Ag nanocomposites." *Surf. Rev. Lett.*, **24**, 1750038 (2017).
45. W. Jilani, N. Fourati, C. Zerrouki, O. Gallot-Lavallée, and H. Guermazi, "Optical, dielectric properties and energy storage efficiency of ZnO/epoxy nanocomposites." *J Inorg Organomet P*, **29**, 456 (2019).
46. H. Ahmed and A. Hashim, "Fabrication of PVA/NiO/SiC nanocomposites and studying their dielectric properties for antibacterial applications." *Egypt J Chem*, **63**, 805 (2020).
47. S. Ebrahim, A. H. Kashyout, and M. Soliman, "Ac and Dc conductivities of polyaniline/poly vinyl formal blend films." *Curr. Appl Phys.*, **9**, 448 (2009).
48. H. Bouaamlat, N. Hadi, and N. Belghiti, "Dielectric properties, AC conductivity, and electric modulus analysis of bulk ethylcarbazole-terphenyl." *Adv. Mater. Sci. Eng.*, **20**, 1 (2020).
49. A. Hashim and A. Hadi, "Novel pressure sensors made from nanocomposites (biodegradable polymers-metal oxide nanoparticles): fabrication and characterization." *Ukr. J. Phys.*, **63**, 754 (2018).
50. E. Abdeltwab and A. Atta, "Influence of ZnO nanoadditives on the structural characteristics and dielectric properties of PVA." *Int J M P B*, **B 35**, 2150310 (2021).